

On advection and diffusion in the mesosphere and lower thermosphere: the role of rotational fluxes

Alexander S. Medvedev and Richard J. Greatbatch

Department of Oceanography, Dalhousie University, Halifax, Canada

R.J. Greatbatch and A.S. Medvedev, Department of Oceanography, Dalhousie University, Halifax, N.S., Canada, B3H 4J1, email: richard.greatbatch@dal.ca, alex.medvedev@dal.ca

Abstract. A formalism to describe the advective and diffusive eddy transport in terms of the mean tracer is presented. It is based on Eulerian averaging, the flux-gradient relation, and the decomposition of the eddy flux of a tracer into advective, diffusive and rotational components. The rotational (non-divergent) flux arises because the conservation equation for the mean tracer contains only a divergence of the eddy flux of the tracer. To provide a closure, a modification to the flux separation technique based on the eddy variance equation is introduced. The “eddy-induced” advective velocity is represented as the sum of two velocities \mathbf{v}_1 and \mathbf{v}_2 . \mathbf{v}_1 is similar to that in the Transformed Eulerian Mean (TEM) formulation but generalized to account for both horizontal and vertical eddy fluxes and mean gradients. The velocity \mathbf{v}_2 depends on the flux of eddy variance of the tracer. The diffusion coefficient is represented as a sum of K_1 , which may serve as a diagnostic of an irreversible mixing, and K_2 , which describes up- or downgradient eddy fluxes of the tracer due to local transformations of the eddy variance. Both \mathbf{v}_2 and K_2 arise from taking account of the rotational fluxes. The scheme is applied to output from a global circulation model of the Middle Atmosphere. It is shown that in the meridional plane, the correction \mathbf{v}_2 to the TEM velocity is small in the mesosphere and lower thermosphere. For the diffusion coefficient, however, the correction K_2 must be accounted for above approximately 110 km.

1. Introduction

Transport in fluids, both advective and non-advective, results from motions on various scales. The common approach in atmospheric and oceanic applications is to subdivide the flow fields and tracer distributions into an average of some sort and deviations (eddies). The effect of the eddies enters the conservation equation for the averaged (mean) tracer through the divergence of the eddy flux of the corresponding tracer. Ultimately, development of a diagnostic for the total transport boils down to finding a relationship between the eddy flux and the mean tracer field.

Material or tracer parcels in the flow experience both translation and deformation. An irreversible deformation and dispersion of parcels at small scales is usually associated with the turbulence and diffusion, while the translation at large scales is considered to occur due to an advection. However, there is no clear distinction between these two processes because an irreversible deformation and mixing of parcels is known to occur even in association with large scale flow (e.g., wave breaking, chaotic advection). Transport phenomena can be studied using Lagrangian-type diagnostics which are designed to follow parcels or contours in the flow. But the Eulerian technique still remains more practical for many applications, because most observations and numerical simulations deal with Eulerian distributions, and the conversion of Lagrangian quantities into the Eulerian ones is not a trivial task [*McIntyre*, 1980]. In this paper we study eddy effects on the transport of the mean tracer in the Eulerian frame of reference.

Since the Eulerian eddy transport encompasses both advection and diffusion of the mean tracer, a flux-gradient relationship,

$$\overline{\mathbf{v}'q'} = -\mathbf{K}\nabla\bar{q}. \quad (1)$$

is commonly assumed, where $\overline{\mathbf{v}'q'}$ is the eddy flux, \mathbf{v}' and q' are the eddy components of the velocity \mathbf{v} and the tracer q , and \mathbf{K} is a tensor. \mathbf{K} can be uniquely decomposed into symmetric and antisymmetric parts and *Plumb* [1979] has shown that the former being associated with a diffusion, and the latter with an advection (skew diffusion). It should be noted that (1) does not define components of the tensor \mathbf{K} unambiguously in 3-dimensional space (9 components of the tensor versus 3 equations), or in a 2-dimensional plane (4 components versus 2 equations). Only in one dimension, can the diffusion coefficient be defined uniquely [*Taylor*, 1915; *Reed and German*, 1965]. Naturally, it would then represent a diffusion rather than advection.

A widely used approach to study large-scale dynamics of the Middle Atmosphere is to consider motions on a 2-dimensional meridional plane by decomposing field variables into zonal mean and zonally asymmetric disturbances (e.g., [*Andrews et al.* 1987]). In earlier studies, the analogy with a small-scale turbulent diffusion was exploited to seek a representation of the eddy flux in the form of the pure diffusive flux of the mean tracer, e.g. [*Reed and German*, 1965]. It soon was recognized that this approximation was poor for large scale eddies, and that the latter contribute also to the net advection of the mean tracer. *Andrews and McIntyre* [1976] suggested a way to approximate the eddy flux of the potential temperature $(\overline{v'\theta'}, \overline{w'\theta'})$ by an advective flux of the mean potential temperature $\bar{\theta}$. They expressed the non-divergent eddy-induced velocity (v^\dagger, w^\dagger) in terms of the streamfunction $\psi = \overline{v'\theta'}/\bar{\theta}_z$. Then the net residual or the Transformed Eulerian

Mean (TEM) circulation is represented by the sum of the Eulerian mean velocity (\bar{v}, \bar{w}) and the eddy induced velocity (v^\dagger, w^\dagger). Note that in deriving the TEM, only the meridional component of the eddy flux was taken into account, and that the diffusive effect of eddy flux was neglected.

Following on from the development of the TEM technique, it was noticed that, besides the advective component, a rotational flux of the form $\nabla \times \mathbf{D}_{eddy}$, where \mathbf{D}_{eddy} is a vector streamfunction, should be included in the eddy flux approximation [*Marshall and Shutts, 1981; McDougall and McIntosh, 1996*]. The latter can be readily understood since the eddy flux appears in the mean tracer conservation equation only in the form of its divergence, and $\nabla \cdot (\nabla \times \mathbf{D}_{eddy}) = 0$. The TEM formalism has since been generalized to account for 3-dimensional mean gradients and eddy fluxes, arbitrary tracer, and any kind the Eulerian averaging, and disturbances of finite amplitude (e.g., [*Nakamura, 2001; Greatbatch, 2001*]).

Projecting $\overline{\mathbf{v}'q'}$ onto the principal axes of the symmetric (diffusive) part of \mathbf{K} in (1), 3 diagonal components representing diffusion coefficients can be found. However, to find the principle axes themselves (or the three remaining elements of the symmetric part of \mathbf{K}), 3 extra equations must be added to close the system. For small amplitude eddies, *Plumb [1979]* suggested to explicitly constrain the components of \mathbf{K} in terms of parcel displacement correlations. When parcel excursions are too long compared to spatial scales of the eddies, their trajectories become intermingled and even stochastic. Therefore, no useful and relevant constraints exist for finite amplitude disturbances. The problem can be simplified by approximating the symmetric part of \mathbf{K} by a locally isotropic diffusion with a single diagonal coefficient. It is a reasonable approximation, because diffusion

along surfaces of constant \bar{q} cannot be distinguished from advective fluxes in the Eulerian frame of reference. *Nakamura* [2001] suggested a diagnostic framework neglecting the rotational flux. His approach is based on a unique decomposition of eddy flux $\overline{\mathbf{v}'q'}$ into vectors normal and parallel to the local surfaces (contours) of constant \bar{q} , the former being attributed to the diffusive component, and the latter associated with the advective (antisymmetric) part of \mathbf{K} . In [*Greatbatch*, 2001], rotational flux is taken into account, and the coefficient of isotropic diffusion is also constrained uniquely (and, incidentally, coincides, for statistically stationary eddies, with that part of the diffusivity *Nakamura* [2001] associates with local, irreversible mixing).

For the stratosphere, it had been shown that the Transformed-Eulerian Mean (or residual) circulation is a good approximation to the advective transport, and to the diabatic circulation (e.g., [*Geller et al.*, 1992]). This success prompted the use of TEM diagnostics in the mesosphere and lower thermosphere (MLT). However, the MLT is somewhat different dynamically from the stratosphere. First, the MLT is subject to a strong cross-isentropic mixing rather than quasi-horizontal stirring, as in the stratosphere. Second, other types of waves comprise eddies in the MLT: tides, gravity waves, nonlinear combinations of harmonics of fast travelling planetary waves. This motivates revisiting the applicability of the TEM formalism to describing eddy effects on the large-scale transport in the MLT. This can be done by explicitly comparing the TEM with the more general approach which we are going to present in this paper. Note that many constituents in the MLT region have very short photochemical lifetimes. When the photochemical timescale is significantly less than the dynamical timescale, then the species is in local photochem-

ical equilibrium, and transport does not enter into the conservation equation, a situation we are not concerned with in this paper.

In section 2 we give a mathematical development of the decomposition of the eddy flux of tracer, $\overline{\mathbf{v}'q'}$, into advective, diffusive and rotational components. The analysis closely follows [Greatbatch, 2001], but, in the process, we introduce a correction to the flux separation closure. In section 3, we apply these results to the fields simulated with a Middle Atmosphere global circulation model COMMA-LIM. These fields serve as a proxy to real motions in the MLT. Discussion and summary are given in Sections 4 and 5, correspondingly.

2. Theory

We begin with the conservation equations for a scalar q and for mass. In the log-pressure coordinates these equations have the form

$$\partial_t(\rho_0 q) + \nabla \cdot (\rho_0 \mathbf{v} q) = Q, \quad (2)$$

$$\nabla \cdot (\rho_0 \mathbf{v}) = 0, \quad (3)$$

where $\mathbf{v} = (u, v, w)$ is the velocity; $\rho_0(z) = \rho_s \exp(-z/H)$ is the background density; $H = RT_s/g$ is the scale height, $T_s(\rho_s)$ being the constant reference temperature (density), R is the gas constant; g is the acceleration of gravity; Q is the source term; operator $\nabla \equiv (\partial_x, \partial_y, \partial_z)$; ∂_i for $i = t, x, y, z$ denote partial derivatives with respect to the corresponding variable. We introduce an arbitrary (temporal, or spatial, or both) Eulerian average and expand variables into the mean and eddy quantities, e.g., $\mathbf{v} = \bar{\mathbf{v}} + \mathbf{v}'$. Taking the average of (2), we obtain

$$\partial_t(\rho_0 \bar{q}) + \nabla \cdot (\rho_0 \bar{\mathbf{v}} \bar{q}) = -\nabla \cdot (\rho_0 \overline{\mathbf{v}'q'}) + \bar{Q}, \quad (4)$$

The corresponding equation for deviations can be derived by subtracting (4) from (2):

$$\partial_t(\rho_0 q') + \nabla \cdot \rho_0 (\mathbf{v}' \bar{q} + \bar{\mathbf{v}} q' + \mathbf{v}' q' - \overline{\mathbf{v}' q'}) = Q'. \quad (5)$$

It is instructive to consider the equations for the mean and eddy variances, $\Phi = \bar{q}^2/2$ and $\bar{\phi} = \overline{q'^2}/2$, respectively. Multiplying (4) by \bar{q} , (5) by q' , averaging, and denoting $\mathcal{D}' = \overline{q' Q'}$ yields

$$\partial_t(\rho_0 \Phi) + \nabla \cdot \rho_0 (\bar{\mathbf{v}} \Phi + \overline{\mathbf{v}' q' \bar{q}}) = \rho_0 \overline{\mathbf{v}' q'} \cdot \nabla \bar{q} + \bar{q} \bar{Q}, \quad (6)$$

$$\partial_t(\rho_0 \bar{\phi}) + \nabla \cdot (\rho_0 \overline{\mathbf{v}' \phi}) = -\rho_0 \overline{\mathbf{v}' q'} \cdot \nabla \bar{q} + \mathcal{D}'. \quad (7)$$

In deriving the above equations we used the mean and eddy mass conservation equations $\nabla \cdot \rho_0 \bar{\mathbf{v}} = 0$ and $\nabla \cdot \rho_0 \mathbf{v}' = 0$, which are the result of (3). In (6) and (7), the terms inside the divergence operator represent the fluxes of mean and eddy variance, respectively; $\mathcal{D}' < 0$ corresponds to a dissipation, and $\mathcal{D}' > 0$ to an injection of the eddy variance $\bar{\phi}$. The term given by the projection of the eddy tracer flux onto the mean gradient, $\overline{\mathbf{v}' q'} \cdot \nabla \bar{q}$, can now be recognized as a conversion rate between the mean and eddy variances. In fact, it is the component of the flux, $\overline{\mathbf{v}' q'}$, that is normal to $\bar{q} = \text{constant}$ surfaces that provides a sink (or a source) for the mean tracer variance. Since diffusion is always associated with a removal of variance, this conversion term provides a motivation to seek a representation of the eddy flux divergence in (4), $\nabla \cdot \rho_0 \overline{\mathbf{v}' q'}$, in the form of a “macro-scale” diffusion. The sign of the conversion rate determines the direction of the exchange between the reservoirs of Φ and $\bar{\phi}$, or the sign of a diffusion coefficient, if the latter is found.

Now we want to approximate the eddy tracer flux by subdividing it into advective, diffusive, and rotational parts following *Greatbatch* [2001]

$$\rho_0 \overline{\mathbf{v}' q'} = \bar{q} \nabla \times \mathbf{B} - \rho_0 \mathbf{K} \nabla \bar{q} + \nabla \times \mathbf{D}, \quad (8)$$

where \mathbf{K} is the symmetric diffusion tensor, \mathbf{B} is the vector streamfunction for the eddy induced velocity $\rho_o \mathbf{v}_{\text{eddy}} = \nabla \times \mathbf{B}$, and the rotational flux $\nabla \times \mathbf{D}$ serves as a gauge because the eddy flux only appears under the sign of $(\nabla \cdot)$ in (4). The first term in the RHS of (8) describes the advective (skew) flux because its divergence can be represented as an advection: $\nabla \cdot (\bar{q} \nabla \times \mathbf{B}) = (\nabla \times \mathbf{B}) \cdot \nabla \bar{q}$. Introducing $\mathbf{T} = \bar{q} \mathbf{B} + \mathbf{D}$ one can rewrite (8) in the form

$$\rho_o \overline{\mathbf{v}'q'} = \mathbf{B} \times \nabla \bar{q} - \rho_o \mathbf{K} \nabla \bar{q} + \nabla \times \mathbf{T}. \quad (9)$$

Since \mathbf{B} appears in (9) in the form $\mathbf{B} \times \nabla \bar{q}$, the component \mathbf{B} parallel to $\nabla \bar{q}$ plays no role. Therefore, without loss of generality we can assume $\mathbf{B} \cdot \nabla \bar{q} = 0$. The solution for \mathbf{B} with this property can be found by taking $\nabla \bar{q} \times$ (9):

$$\mathbf{B} = |\nabla \bar{q}|^{-2} \nabla \bar{q} \times \left(\rho_o \overline{\mathbf{v}'q'} + \rho_o \mathbf{K} \nabla \bar{q} - \nabla \times \mathbf{T} \right). \quad (10)$$

Taking the scalar product of $\nabla \bar{q}$ with (9) yields

$$\rho_o \overline{\mathbf{v}'q'} \cdot \nabla \bar{q} = -\rho_o \nabla \bar{q} \cdot \mathbf{K} \nabla \bar{q} + \nabla \cdot (\mathbf{T} \times \nabla \bar{q}). \quad (11)$$

As seen from (11), both diffusive and rotational components of the eddy flux of the tracer project onto the mean gradient $\nabla \bar{q}$, and therefore affect the rate of conversion of the mean tracer variance Φ into the eddy variance $\bar{\phi}$. The advective part of the flux described by \mathbf{B} is conservative in the sense that it only redistributes Φ , but does not convert it into $\bar{\phi}$. Note that in [Nakamura, 2001], the term $\rho_o \overline{\mathbf{v}'q'} \cdot \nabla \bar{q}$ was approximated entirely through the diffusive flux.

Our next step is to solve for \mathbf{K} and \mathbf{T} . Equating $\rho_o \overline{\mathbf{v}'q'} \cdot \nabla \bar{q}$ from (7) and (11), we obtain

$$\nabla \cdot (\rho_o \overline{\mathbf{v}\phi} + \mathbf{T} \times \nabla \bar{q} + \nabla \times \mathbf{G}) = \rho_o \nabla \bar{q} \cdot \mathbf{K} \nabla \bar{q} + (\mathcal{D}' - \partial_t \rho_o \bar{\phi}), \quad (12)$$

where \mathbf{G} is another gauge vector. *Greatbatch* [2001] proposed a generalization of the flux decomposition of *Marshall and Shutts* [1981]. In particular, it was suggested to associate the diffusive part, $\rho_0 \nabla \bar{q} \cdot \mathbf{K} \nabla \bar{q}$ with the local, irreversible removal of the variance $\bar{\phi}$ by a small-scale diffusion (and/or a reversible change due to a non-stationarity), and the rotational part with the advection of the eddy variance. Mathematically, this assumption allows one to equate the left- and right-hand sides of (12) to zero separately:

$$\mathbf{T} \times \nabla \bar{q} = -\rho_0 \overline{\mathbf{v} \phi}, \quad (13)$$

$$\rho_0 \nabla \bar{q} \cdot \mathbf{K} \nabla \bar{q} = \partial_t \rho_0 \bar{\phi} - \mathcal{D}', \quad (14)$$

where in (13) we put $\mathbf{G} = 0$. It is necessary to emphasize that the above flux decomposition is only an assumption which allows us to obtain the two equations (13) and (14), and as such it is not unique. Note that (13) is applicable to finite amplitude eddies because $\overline{\mathbf{v} \phi} = \bar{\mathbf{v}} \bar{\phi} + \overline{\mathbf{v}' \phi}$.

In this paper we realize that there is a deficiency in the decomposition (13) and (14), and suggest a way to modify it. In order to demonstrate this, we integrate (12) over the volume inside a closed \bar{q} surface. This is certainly applicable to horizontal or meridional planes in two dimensions. In the meridional plane, if the contour is not closed the integration should be performed from pole to pole between two different contours $\bar{q} = \text{const}$. Denoting the area of integration by V and the corresponding bounding surface by S , we obtain

$$\int_S \rho_0 \overline{\mathbf{v} \phi} \cdot \hat{\mathbf{n}} dS = \int_V \rho_0 \nabla \bar{q} \cdot \mathbf{K} \nabla \bar{q} dV + \int_V (\mathcal{D}' - \partial_t \rho_0 \bar{\phi}) dV, \quad (15)$$

where $\hat{\mathbf{n}} = \nabla \bar{q} / |\nabla \bar{q}|$ is the unit vector normal to the surface. As seen from (15), the variance flux $\overline{\mathbf{v} \phi}$ cannot entirely be attributed to the rotational part $\mathbf{T} \times \nabla \bar{q}$, as in (13), because $\int_S \mathbf{T} \times \nabla \bar{q} \cdot \hat{\mathbf{n}} dS = 0$. In other words, (15) represents an integral rate of conversion

between the tracer variances Φ and $\bar{\phi}$ inside the volume V (cf. (11)). Unless the volume V covers the entire domain of integration with no variance fluxes across the outer boundaries, the components of the flux $\rho_0 \overline{\mathbf{v}\phi}$ normal to the surface S contribute to this rate of change. As a result, variance fluxes contribute to the integral conversion rate between Φ and $\bar{\phi}$ represented by the second term in (15), and, consequently to \mathbf{K} . To account for this, we partition the eddy variance flux into components normal and parallel to the isosurface \bar{q}

$$\rho_0 \overline{\mathbf{v}\phi} = \alpha \nabla \bar{q} + \mathbf{b} \times \nabla \bar{q}. \quad (16)$$

This expansion is unique, and the coefficient α and the vector \mathbf{b} are given by

$$\alpha = |\nabla \bar{q}|^{-2} (\rho_0 \overline{\mathbf{v}\phi} \cdot \nabla \bar{q}), \quad \mathbf{b} = |\nabla \bar{q}|^{-2} (\nabla \bar{q} \times \rho_0 \overline{\mathbf{v}\phi}). \quad (17)$$

The decomposition (13) and (14) can now be modified to associate the divergence of the flux of eddy variance that is normal to surfaces $\bar{q} = \text{const}$ with the large-scale diffusion of \bar{q} , and the part of $\rho_0 \overline{\mathbf{v}\phi}$ tangential to $\bar{q} = \text{const}$ surfaces with the “rotational” flux $\mathbf{T} \times \nabla \bar{q}$:

$$\mathbf{T} = -\mathbf{b}, \quad (18)$$

$$\rho_0 \nabla \bar{q} \cdot \mathbf{K} \nabla \bar{q} = \partial_t \rho_0 \bar{\phi} - \mathcal{D}' + \nabla \cdot \alpha \nabla \bar{q}. \quad (19)$$

Thus, we have a closed set of equations for determining the vector streamfunction \mathbf{B} provided that the symmetric macro-scale “diffusion” tensor \mathbf{K} is known: (10), (17), and (18). This is not the case for \mathbf{K} because all the components of the tensor cannot be found unambiguously from the only equation (19). However, it is convenient to introduce an assumption that the eddy diffusion is isotropic, i.e., $\mathbf{K} = K\mathbf{I}$, where \mathbf{I} is the unit matrix. This allows a unique definition for the only eddy diffusion coefficient K from (19):

$$K = \rho_0^{-1} |\nabla \bar{q}|^{-2} (\partial_t \rho_0 \bar{\phi} - \mathcal{D}' + \nabla \cdot \alpha \nabla \bar{q}). \quad (20)$$

In the introduced diagnostics, $\nabla \cdot \alpha \nabla \bar{q}$ in (20) is the new term compared to *Greatbatch* [2001] in the definition of K , although the expression (18) for the rotational streamfunction \mathbf{T} is the same as in *Greatbatch* [2001]. In *Nakamura* [2001], the divergence of the entire variance flux is associated with K , and no rotational component contribution to the advective streamfunction \mathbf{B} is given. Note that $K > 0$ implies transfer down the mean gradient $\nabla \bar{q}$. It follows that local growth of eddy variance, $\partial_t \rho_0 \bar{\phi} > 0$, results in transport down the mean gradient, as does the local irreversible removal of $\bar{\phi}$, $-\mathcal{D}' > 0$. On the other hand, the divergence of the flux of eddy variance normal to iso-surfaces (contours) of \bar{q} can have either sign: divergence contributes to the downgradient transfer of \bar{q} , and convergence to the upgradient transfer of \bar{q} .

The assumption of isotropic diffusion also simplifies (10): the term containing $K \nabla \bar{q}$ drops out since $\nabla \bar{q} \times K \nabla \bar{q} = 0$. With (18) this gives the equation for the vector streamfunction \mathbf{B} :

$$\mathbf{B} = |\nabla \bar{q}|^{-2} \nabla \bar{q} \times \left(\rho_0 \overline{\mathbf{v}'q'} + \nabla \times \mathbf{b} \right) \equiv \mathbf{B}_1 + \mathbf{B}_2. \quad (21)$$

In (21) we introduced the notations \mathbf{B}_1 for the part of the streamfunction \mathbf{B} associated with the flux $\rho_0 \overline{\mathbf{v}'q'}$, and \mathbf{B}_2 for the part due to $\nabla \times \mathbf{b}$, or, in turn, due to the variance flux $\rho_0 \overline{\mathbf{v}\phi}$. Now the eddy induced velocity can be found from the streamfunction \mathbf{B} :

$$\rho_o \mathbf{v}_{\text{eddy}} = \nabla \times \mathbf{B} = \nabla \times \mathbf{B}_1 + \nabla \times \mathbf{B}_2 \equiv \rho_o \mathbf{v}_1 + \rho_o \mathbf{v}_2, \quad (22)$$

where \mathbf{v}_1 is the eddy velocity component due to the flux $\rho_0 \overline{\mathbf{v}'q'}$ in (21), and \mathbf{v}_2 is due to the flux of eddy variance $\rho_0 \overline{\mathbf{v}\phi}$. These velocities should be added to the Eulerian-mean velocity, $\bar{\mathbf{v}}$, to obtain the net transport velocity for the tracer \bar{q} , \mathbf{v}^* :

$$\mathbf{v}^* = \bar{\mathbf{v}} + \mathbf{v}_{\text{eddy}} = \bar{\mathbf{v}} + \mathbf{v}_1 + \mathbf{v}_2. \quad (23)$$

\mathbf{v}_1 is related to the eddy induced velocity introduced in TEM (but generalized since we use $\nabla\bar{q}$ in (21), rather than the vertical gradient of \bar{q}), whereas \mathbf{v}_2 appears as a correction associated with the rotational component of the eddy flux.

3. Results from the numerical model

In this section we apply the diagnostic framework presented above to the fields simulated with the COMMA-LIM (Cologne Model of the Middle Atmosphere - Leipzig Institute for Meteorology). It is a three-dimensional finite-difference global circulation model extending up from 0 to slightly above 135 km with a log-pressure vertical coordinate $z = -H\ln(p/p_s)$, where $H = 7$ km and p_s is the reference pressure at the lower boundary. The model has 64 grid points in the longitude direction, 36 in the latitude, and 48 in the vertical which represents resolution of approximately 5° in the horizontal and 2.87 km in the vertical. Details of the model's architecture can be found in [Fröhlich *et al.*, 2003]. The results we are to analyze were simulated for perpetual July. After the initial spin-up to establish an almost equilibrium state, the model was run for an additional 10 days to collect data with time interval of 2 hours. This was done in order to have a good temporal resolution for eddies. Among those in the (MLT), the most persistent are the solar tide, stationary and various travelling planetary waves.

Figure 1 presents a zonal mean distribution of the simulated temperature (upper panel), and the corresponding monthly mean climatology for July from the COSPAR International Reference Atmosphere (CIRA) (lower panel). It is seen that the model successfully reproduces the raised winter stratopause, very cold summer mesopause (although almost 20 degrees warmer than in CIRA), and the overall temperature distribution. The latter is mostly determined by the meridional circulation and eddy motions including the param-

eterized ones. Comparison of other elements of the model circulation like tides, planetary waves, zonal mean wind with observations also shows that the COMMA-LIM reproduces the circulation of the Middle Atmosphere reasonably well [Fröhlich *et al.*, 2003]. Thus, the simulated fields can serve as a proxy for the circulation of the real Middle Atmosphere.

In what follows, the averaging operator consists of a time average over the last 10 days of integration (after the model has reached an equilibrium state corresponding to the monthly mean July) followed by a zonal average. All formulae from the previous section can easily be converted to this two-dimensional case by putting $\partial_x \overline{\{\cdot\}} = 0$, and considering only x -components of the vector streamfunctions: e.g., $\mathbf{B} = (B, 0, 0)$, $\mathbf{T} = (T, 0, 0)$, $\mathbf{b} = (\beta, 0, 0)$. More explicit expressions are given in the Appendix. We apply the diagnostics from the previous section to the transport of the potential temperature ($q \equiv \theta$), since, first, the latter is the fundamental quantity in geophysical fluid dynamics, and second, because it allows a direct comparison with the residual circulation of *Andrews and McIntyre* [1976]. There are strong radiative sources and sinks for the potential temperature in the atmosphere, and therefore, it cannot be considered as an exactly conservative scalar. The results will be shown in the global domain extending from $z=65$ to 125 km covering the mesosphere and lower thermosphere. Note that the top altitude is approximately one standard atmospheric height below the upper boundary of the domain of integration. Thus we significantly reduce a contamination of the fields associated with the reflection at the top levels of the model.

The latitude-altitude cross-section of the zonal mean potential temperature, $\bar{\theta}$, is presented in Figure 2a. Note that it has an order of tens thousand K's in the MLT because of the exponential growth with height: $\theta = T \exp(\kappa z/H)$, where T is the temperature as in

Figure 1, $\kappa = R/c_p$, c_p is the specific heat at constant pressure. It is seen that the lines of constant $\bar{\theta}$ are mostly horizontal, especially in the thermosphere. Below the mesopause, the isolines are tilted downward from the summer hemisphere toward the winter hemisphere as a result of seasonal differences in radiative sources. Meridional and vertical fluxes of potential temperature due to resolved eddies, $\overline{v'\theta'}$ and $\overline{w'\theta'}$, are shown in Fig 2b and 2c, correspondingly. The meridional heat flux is mostly poleward in the both hemispheres, has a more complex structure near the equator, and its magnitude varies from -1.5×10^5 to 3×10^5 m s⁻¹K. The vertical flux is downward practically throughout the entire Middle Atmosphere with the magnitude of -1.4×10^3 m s⁻¹K in the tropical lower thermosphere. This structure of the potential temperature fluxes with peaks centered around the equator occurs mostly due to the diurnal and semidiurnal tides.

Besides the fluxes associated with resolved eddies, those due to unresolved subgrid-scale motions must also be taken into account. In the Middle Atmosphere, these are primarily associated with parameterized gravity waves (GW). For any GW drag scheme employed by the model, the eddy flux of temperature can be estimated using formulae (42) and (43) of *Medvedev and Klaassen* [2003]. Since horizontal propagation of gravity waves is commonly neglected in GW drag parameterizations, including the multiple-wave Lindzen scheme utilized here, only the vertical component of the eddy flux of potential temperature, $\overline{w'\theta'}_{GW}$, should be considered. It is plotted in Figure 2d. Most of the potential temperature flux due to parameterized gravity waves is concentrated in midlatitudes in both hemispheres with stronger fluxes in the winter hemisphere (peak values up to 140 m s⁻¹K near the mesopause). This pattern forms because stronger filtering of both eastward and westward travelling GW harmonics in the summer hemisphere considerably

reduces fluxes of propagating gravity waves in the MLT. Overall, $\overline{w'\theta'}_{GW}$ exceeds fluxes due to resolved waves below approximately 110 km, but the latter significantly dominate above. In our calculations ahead, we shall use the sum of the fluxes shown in Figure 2c and 2d. It is seen from the Fig. 2 that the eddy fluxes of potential temperature are mainly directed down the gradient of the mean potential temperature, $\nabla\bar{\theta}$. Indeed, calculations (not shown here) render the conversion term in the RHS of (6) and (7), $\rho_0\overline{\mathbf{v}'\theta'} \cdot \nabla\bar{\theta}$, negative almost everywhere in the MLT. Therefore, in the meridional plane, eddies provide mainly a sink of the variance of the mean potential temperature, $\Phi = \bar{\theta}^2/2$, (or the available mean potential energy) into the reservoir of eddy variance $\bar{\phi} = \bar{\theta'^2}/2$ (or the available eddy potential energy). This agrees well with the concept of large-scale diffusion induced by eddies.

Horizontal and meridional fluxes of eddy variance, $\overline{v\phi}$ and $\overline{w\phi}$, are depicted in Figure 3a and 3b, correspondingly. We remind the reader that v and w are the full velocities which include both mean and eddy components. It is seen from the figure that these fluxes are concentrated in the tropics since the eddy motions at low latitudes associated with the solar tide and travelling planetary waves are stronger there. The magnitude of $\overline{v\phi}$ varies from -15 to 18 m s⁻¹K², and from -0.08 to 0.05 m s⁻¹K² for $\overline{w\phi}$, and they form a complex set of cells. Figure 3c presents the “rotational” streamfunction, $T = -|\nabla\bar{\theta}|^{-2}\rho_0(\overline{w\phi\partial_y\bar{\theta}} - \overline{v\phi\partial_z\bar{\theta}}) \equiv -\beta$, calculated using (17) and (18). As follows from (21), the curl of $\mathbf{T} = (T, 0, 0)$ must be added to the eddy flux $\rho_0\overline{\mathbf{v}'\theta'}$ in order to calculate the total eddy streamfunction B . This flux associated with the transport of eddy variance is pointed along the lines of constant T , such that local minima of T lie to the right (and the local maxima to the left) of its direction. Fig. 3c shows that the “rotational” flux

forms a set of cells that alternate with height and are tilted downward and towards the equator.

The components of the advective streamfunction are plotted in Figure 4. The streamfunction associated with the advection by the zonal mean motions,

$$\rho_o \bar{\mathbf{v}} = \rho_o(0, \bar{v}, \bar{w}) = \nabla \times (B_{Eul}, 0, 0), \quad (24)$$

is given in Figure 4a. It is seen that the Eulerian-mean transport is mostly cross-hemispheric with a strong clockwise cell near the equator. Descending and ascending motions near the poles are mostly due to the Eulerian mean radiative cooling and heating in the winter and summer hemispheres, respectively. The part of the eddy induced streamfunction associated with the heat flux $\rho_o \overline{\mathbf{v}'\theta'}$, B_1 , is plotted in Fig. 4b. This part is similar to the eddy-induced portion of the residual circulation in the Transformed Eulerian-mean formalism of *Andrews and McIntyre* [1976]. Scale analysis of the components $B_1 = \rho_o |\nabla \bar{\theta}|^{-2} (\overline{w'\theta'} \partial_y \bar{\theta} - \overline{v'\theta'} \partial_z \bar{\theta})$ (see also (28)) shows that $\overline{w'\theta'} \ll \overline{v'\theta'}$ and $\partial_y \bar{\theta} \ll \partial_z \bar{\theta}$, such that $B_1 \approx \rho_o (\partial_z \bar{\theta})^{-1} \overline{v'\theta'}$. The latter expression coincides with the one for the TEM streamfunction [*Andrews et al.*, 1987]. The circulation it describes is purely due to eddy motions, and is directed mostly against the Eulerian-mean, \bar{B} . The part of the eddy induced streamfunction associated with the “rotational” flux correction, B_2 , is shown in Fig 4c. It does not exactly follow the streamfunction T , but clearly has similar structure: the series of tilted cells concentrated near the equator. This part of the advective circulation is primarily caused by thermal tides which are strong in the model. Scaling analysis of B_2 using data from Fig. 2 and 3 shows that $B_2 \approx (\partial_z \bar{\theta})^{-1} \partial_z [\rho_o \overline{\mathbf{v}'\phi} (\partial_z \bar{\theta})^{-1}]$, which coincides with the expression for the Temporal Residual Mean rotational streamfunction of *McDougall and McIntosh* [1996]. The total residual streamfunction, the sum

of \bar{B} , B_1 and B_2 , is plotted in Figure 4d. It represents mainly the pole-to-pole transport from the summer hemisphere into the winter one. The strong equatorial circulation cell in the Eulerian-mean circulation is being canceled mainly by B_1 , as in the stratosphere [Andrews *et al.*, 1987]. The “rotational” component of the streamfunction B_2 plays a minor role compared to B_1 throughout the domain of integration. The contribution of all parts of the advective circulation can be seen in more details in Figure 5 where the corresponding components of the meridional transport velocity $v^* = \bar{v} + v_1 + v_2$ are plotted at $z \approx 110\text{km}$. Here the velocities are defined as follows (see also Appendix):

$$\rho_o(0, v_1, w_1) = \nabla \times (B_1, 0, 0), \quad \rho_o(0, v_2, w_2) = \nabla \times (B_2, 0, 0). \quad (25)$$

The velocity v_1 induced by the eddy heat flux $\rho_0 \overline{\mathbf{v}'\theta'}$ has a comparable magnitude (up to 11 m s^{-1}) as the Eulerian-mean one, \bar{v} , (the peak value is 21 m s^{-1}), but directed mostly opposite. The velocity v_2 due to the eddy flux of heat variance, $\rho_0 \overline{\mathbf{v}'\phi}$, is several times smaller (3.5 m s^{-1} in the maximum) than \bar{v} and v_1 . Its direction may either coincide with v_1 (as in the Northern Hemisphere), or be the opposite (as in the Southern Hemisphere).

The diffusion coefficient K can be evaluated using (20) under the steady state condition ($\partial_t \rightarrow 0$)

$$K = \rho_0^{-1} |\nabla \bar{q}|^{-2} (-\mathcal{D}' + \nabla \cdot \alpha \nabla \bar{q}) \equiv K_1 + K_2, \quad (26)$$

where the nonhomogeneous source/sink term \mathcal{D}' is calculated from (7) and $\partial_t \rightarrow 0$. In (26) we split K into two parts, K_1 and K_2 , associated with \mathcal{D}' , and with the divergence of the component of the flux of eddy variance flux that is normal to isolines of $\bar{\theta}$, respectively. The diffusion coefficient K_1 is the same as in Nakamura [2001] and Greatbatch [2001]. It attributes the small-scale dissipation of eddy variance, \mathcal{D}' , to the macro-scale diffusion. As

seen from Figure 6a, K_1 is positive almost everywhere in the domain. This is because the main diabatic effect on eddies is radiative damping, i.e. $\mathcal{D}' < 0$. The diffusion coefficient K_1 has magnitude of several hundred of $\text{m}^2 \text{s}^{-1}$ in the MLT and increases with height. The magnitude and vertical distribution are consistent with those observed by *Lübken* [1997, Figure 4], those estimated theoretically by *Chandra* [1980, Figure 4] for momentum eddy diffusivity, and those obtained in the simulations with the middle atmosphere GCM with parameterized gravity waves for the thermoconductivity by *Medvedev and Klaassen* [2003, Figure 7]. Comparison with eddy fluxes in Figure 2 shows that the equatorial maximum of K_1 is mainly due to the resolved eddies, while the two midlatitude peaks at ≈ 95 km largely result from the parameterized gravity waves.

Contrary to K_1 , the coefficient K_2 has alternating signs, as depicted in Figure 6b. It is seen from Figure 3a and 3b that the component of the flux of eddy variance that is normal to isolines $\bar{\theta}=\text{const}$ has either sign, as does its divergence, $\nabla \cdot \alpha \nabla \bar{q}$, and therefore K_2 (which in our case is still lower than the upper boundary of the domain of integration). The magnitude of K_2 rises sharply with height. It varies from -2500 to 3000 $\text{m}^2 \text{s}^{-1}$ near the top of the domain. The latitudinal cross-sections of the diffusion coefficient K and its components K_1 and K_2 at $z=110$ and 120 km are shown in Figure 7. The altitude 110 km is where K_1 and K_2 have about the same magnitude, albeit a similar latitudinal structure with an equatorial peak, two weaker maxima at higher latitudes, and the corresponding minima in between. Below 110 km, the contribution of K_2 to K can be neglected. Above this height, K_2 clearly dominates K_1 , as seen in Figure 7b.

4. Discussion

Although non-unique, diagnosis of transport in the form of advection and diffusion based on the representation of the eddy fluxes in the flux-gradient form (1) is quite useful and practical. Perhaps, the Transformed Eulerian Mean (TEM) is the most widely used example of this formalism in atmospheric applications. Such diagnostic implies that the eddy flux of the tracer can be subdivided into advective and diffusive components. The advective part describes a transport of the mean tracer by an “eddy-induced” non-divergent velocity. The diffusive part is associated with a removal (or injection, in the case of “negative” diffusion) of Φ , and represents an eddy flux of tracer along the principal axes of the symmetric part of \mathbf{K} . The direction of the diffusive flux necessarily projects onto the mean gradient $\nabla\bar{q}$. The non-uniqueness of such diagnostics shows up mathematically in the fact that the tensor \mathbf{K} has more components than the equations to define them (unless in the one-dimensional case). Physically, the ambiguity of the flux-gradient relation presents itself as a lack of criteria to differentiate between the advective and diffusive transport in the direction along the iso-surfaces in the Eulerian frame of reference. Approaches based on Lagrangian-type averaging have been proposed to circumvent this problem, e.g., [Nakamura, 1996; Haynes and Shuckburgh, 2000]. However, in this paper we consider only the transport diagnostics based on the Eulerian averaging and flux-gradient relation (1).

A schematic representation of the tracer variance conversion is given by (6) and (7), and is illustrated in the box diagram of Figure 8. Diagrams of this sort are often used to visualize exchanges between the eddy and “mean” components of energy, the other quadratic quantity of field variables. The reservoirs Φ and $\bar{\phi}$ denote the mean and eddy variances, respectively, contained in an infinitesimal volume dV . The conversion term

appears as an “eddy induced” source/sink with respect to the mean variance Φ . It is represented in (11) and in the diagram by the (i) diffusive and (ii) rotational fluxes. On the other hand, the conversion is determined by the balance between the small-scale source/sink \mathcal{D}' , the transience (if the eddies are statistically unsteady), and the divergence of the eddy variance flux. When integrated over the volume between two surfaces, $\bar{q} = \text{constant}$, the term (ii) associated with the rotational flux does not contribute to the variance conversion, and neither does the tangential component of $\rho_0 \overline{\mathbf{v}\phi}$ (also denoted by (ii) in Figure 8). In the paper, we used this property to equate the terms marked by (ii) to provide a required closure.

Using simulations with the global circulation model COMMA-LIM, we have shown that for potential temperature in the meridional plane in the MLT, the main effect of \mathcal{D}' is radiative damping, i.e. $\mathcal{D}' < 0$. The components of the eddy variance flux $\rho_0 \overline{\mathbf{v}\theta'^2}/2$ have either sign, as does its divergence. This means that the part of the total diffusion coefficient determined by \mathcal{D}' , K_1 in (26), is always positive, whereas the other part, K_2 , can have both signs. Thus, K_1 describes a downgradient transport of the mean potential temperature which removes its mean variance, and ultimately, channels it out of the system through the radiative cooling \mathcal{D}' . Only K_1 serves as a diagnostic of an irreversible mixing of $\bar{\theta}$ due to zonally asymmetric eddies. K_2 describes a reversible conversion of the mean variance due to local transformations of the eddy variance. In an insulated system (with no fluxes through the boundaries), the “diffusion” associated with K_2 does not change the total mean variance in the volume.

One aspect which needs to be mentioned is that the tracer transport velocity and diffusivity obtained within the presented diagnostic framework depend on the structure

of the tracer distribution, or more precisely, on the distribution of the mean tracer and eddy correlations $\overline{\mathbf{v}'q'}$ and $\overline{\mathbf{v}\phi}$. This raises a question of whether the transport and mixing are the properties of the flow, or the functions of a particular tracer. There are indications that initially uncorrelated tracers tend to form a linear compact relation [*Plumb and Ko*, 1992], thus yielding the same velocities and diffusivities for all the tracers. However, one can only expect compact relationships between fairly long-lived tracers for which the transport effects can largely determine the shape of the tracer distributions. It is unlikely that many constituents in the MLT (where photochemical lifetimes are generally very short) would satisfy this. Clearly, this problem is out of the scope of the present paper. Further scrutiny is required to answer the question: When (or if at all) the same K -tensor could be applied to describe the eddy transport of many tracers.

5. Summary

We present a formalism to describe the eddy transport in terms of the mean tracer. It is based on the Eulerian averaging and flux-gradient relation (1). Following *Greatbatch* [2001], we decompose the eddy flux of the tracer into advective, diffusive, and rotational parts. The mean tracer conservation equation contains only a divergence of the eddy flux, and therefore, any non-divergent function can generally be added to a particular solution to satisfy the equation. The rotational flux arises as such a function, or gauge. To provide a closure, we employ a flux-separation technique similar to that of *Marshall and Shutts* [1981]. In this paper, we introduce a modification to the technique, extending that used by *Greatbatch* [2001]. Instead of attributing the rotational flux to the entire flux of eddy variance $\overline{\mathbf{v}\phi}$, we associate the component of $\overline{\mathbf{v}\phi}$ that is tangential to surfaces $\bar{q} = \text{const}$ with the rotational flux, and the normal component of $\overline{\mathbf{v}\phi}$ with the diffusive part of $\overline{\mathbf{v}'q'}$.

In the core of this modification lies the observation that only a component of the eddy variance flux directed along the mean gradient contributes to the conversion between the mean and eddy variances in a finite volume V bounded either by a surface of constant \bar{q} or two surfaces $\bar{q} = \text{constant}$.

We obtained an expression (21) for the advective streamfunction \mathbf{B} which is the sum of the TEM streamfunction \mathbf{B}_1 (but more general than in [*Andrews and McIntyre, 1976*]), and the rotational component \mathbf{B}_2 . The latter is similar to the one derived within the framework of Temporal Residual-Mean [*McDougall and McIntosh, 1996*], and is the same as in [*Greatbatch, 2001*]. The rotational part is not considered in the diagnostic scheme of *Nakamura* [2001]. The corresponding transport velocities \mathbf{v}_1 and \mathbf{v}_2 are given by (22). While \mathbf{v}_1 is expressed in terms of eddy fluxes $\overline{\mathbf{v}'q'}$ (similar to the TEM), the component \mathbf{v}_2 accounts for the flux of eddy variance of the tracer $\overline{\mathbf{v}q'^2}$. For the diffusive flux, we obtain a diffusion coefficient (20). It can be represented through the sum of K_1 and K_2 , where K_2 results from the modification of the eddy flux decomposition, and is a function of the flux of eddy variance.

In this paper, we explicitly evaluate the transport velocities \mathbf{v}_1 and \mathbf{v}_2 given by (25), and components of the diffusion coefficient K_1 and K_2 for the zonal mean potential temperature from the fields simulated with the COMMA-LIM. It is demonstrated that K_2 can be neglected with respect to K_1 below approximately 110 km, but its contribution to the total diffusion coefficient dominates above this height. We show that the component of the eddy induced velocity associated with the rotational flux, \mathbf{v}_2 , represents a smaller correction to the conventional Transformed Eulerian-Mean velocity, and therefore can be ignored in the MLT below at least 125 km.

Appendix

As was suggested by a reviewer, here we provide the explicit formulae applicable for the zonally averaged fields in the 2-dimensional meridional plane.

The vector streamfunctions \mathbf{B} and \mathbf{b} in (21) are then reduced to the scalar streamfunctions $B = B_1 + B_2$ and β , respectfully. Using the letter subscripts as the notations for the corresponding partial derivatives in this Appendix only, we obtain from (17)

$$\beta = \frac{1}{(\bar{q}_y)^2 + (\bar{q}_z)^2} (\rho_0 \overline{w\phi\bar{q}_y} - \rho_0 \overline{v\phi\bar{q}_z}), \quad (27)$$

where $\phi = \overline{q'^2}/2$ is the eddy variance, and $v = \bar{v} + v'$, $w = \bar{w} + w'$ are the full velocities.

Then, from (21), we have

$$B_1 = \frac{1}{(\bar{q}_y)^2 + (\bar{q}_z)^2} (\rho_0 \overline{w'q'\bar{q}_y} - \rho_0 \overline{v'q'\bar{q}_z}), \quad (28)$$

$$B_2 = -\frac{1}{(\bar{q}_y)^2 + (\bar{q}_z)^2} (\beta_y \bar{q}_y + \beta_z \bar{q}_z). \quad (29)$$

The meridional components of the eddy induced velocity can be written using (22):

$$v_{eddy} = v_1 + v_2 = \rho_0^{-1} (B_1)_z + \rho_0^{-1} (B_2)_z, \quad (30)$$

$$w_{eddy} = w_1 + w_2 = -\rho_0^{-1} (B_1)_y - \rho_0^{-1} (B_2)_y. \quad (31)$$

Acknowledgments. We thank Dr. Alex Pogoreltsev for providing us the results of simulations with COMMA-LIM. Comments made by three anonymous referees helped to improve the presentation in the paper. Funding from NSERC, CFCAS and CICS is gratefully acknowledged.

References

Andrews, D.G., J.R. Holton, and C.B. Leovy. *Middle Atmosphere Dynamics*, Academic Press, 1987.

- Andrews, D.G., and M.E. McIntyre. Planetary waves in horizontal and vertical shear: The generalized Eliassen-Palm relation and the mean zonal acceleration. *J. Atmos. Sci.*, *33*, 2031-2048, 1976.
- Chandra, S. Energetics and thermal structure of the middle atmosphere. *Planet. Space Sci.*, *28*, 585-593, 1980.
- Fröhlich, K., A. Pogoreltsev, and Ch. Jacobi. The 48 layer COMMA-LIM model: Model description, new aspects, and climatology. *Wiss. Mitt. Inst. f. Meteorol. Univ. Leipzig*, *30*, 149-185, 2003.
- Geller, M.A., E.R. Nash, M.F Wu, and J.E. Rosenfield. Residual circulations calculated from satellite data: their relations to observed temperature and ozone distributions. *J. Atmos. Sci.*, *49*, 1127-1137, 1992.
- Greatbatch, R.J. A framework for mesoscale eddy parameterization based on density-weighted averaging at fixed height. *J. Phys. Oceanogr.*, *31*, 2797-2806, 2001.
- Haynes, P.H., and E. Shuckburgh. Effective diffusivity as a diagnostic of atmospheric transport. 1. Stratosphere. *J. Geophys. Res.*, *105*, 22,777-22,794, 2000.
- Lübken, F.-J. Seasonal variation of turbulent energy dissipation rates at high latitudes as determined by in situ measurements of neutral density fluctuations. *J. Geophys. Res.*, *102*, 13,441-13,456, 1997.
- Marshall, J., and G. Shutts. A note on rotational and divergent eddy fluxes. *J. Phys. Oceanogr.*, *11*, 1677-1680.
- McDougall, T.J., and P.C. McIntosh. The temporal-residual-mean velocity. Part I: Derivation and the scalar conservation equations. *J. Phys. Oceanogr.*, *26*, 2653-2665, 1996.

- McIntyre, M.E. Towards a Lagrangian-mean description of stratospheric circulations and chemical transports. *Philos. Trans. R. Soc. London, Ser. A 296*, 129-148, 1980.
- Medvedev, A.S., and G.P. Klaassen. Thermal effects of saturating gravity waves in the atmosphere. *J. Geophys. Res.*, *108*(D2), 4040, doi:10.1029/2002JD002504, 2003.
- Nakamura, N. Two-dimensional mixing, edge formation, and permeability diagnosed in an area coordinate. *J. Atmos. Sci.*, *53*, 1524-1537, 1996.
- Nakamura, N. A new look at eddy diffusivity as a mixing diagnostic. *J. Atmos. Sci.*, *58*, 3685-3701, 2001.
- Plumb, R.A. Eddy fluxes of conserved quantities by small-amplitude waves. *J. Atmos. Sci.*, *36*, 1699-1704, 1979.
- Plumb, R.A., and M.K.W. Ko. Interrelationships between mixing ratios of long-lived stratospheric constituents. *J. Geophys. Res.*, *97*, 10145-10,156, 1992.
- Reed, R.J., and K.E. German. A contribution to the problem of stratospheric diffusion by large-scale mixing. *Mon. Wea. Rev.*, *93*, 313-321, 1965.
- Taylor, G.I. Eddy motions in the atmosphere. *Philos. Trans. Roy. Soc. London, A215*, 1-26, 1915.

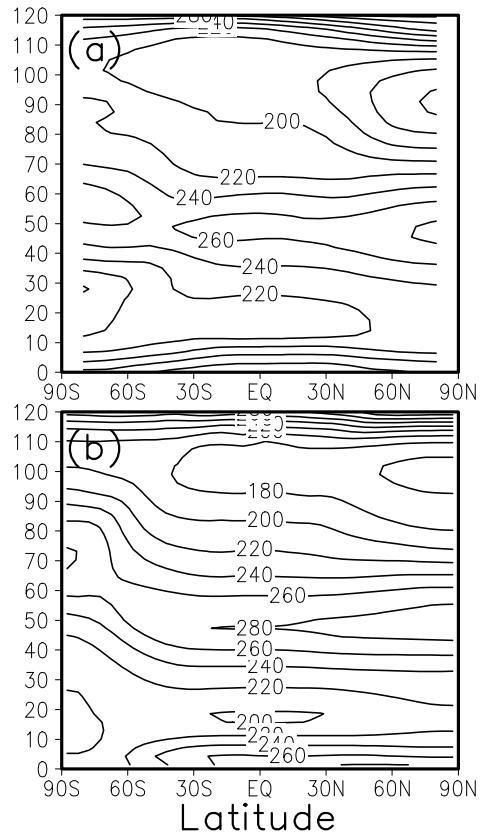


Figure 1. Zonal mean temperature simulated in the COMMA-LIM (upper panel), and monthly mean temperature from CIRA for July. Contour interval is 20K.

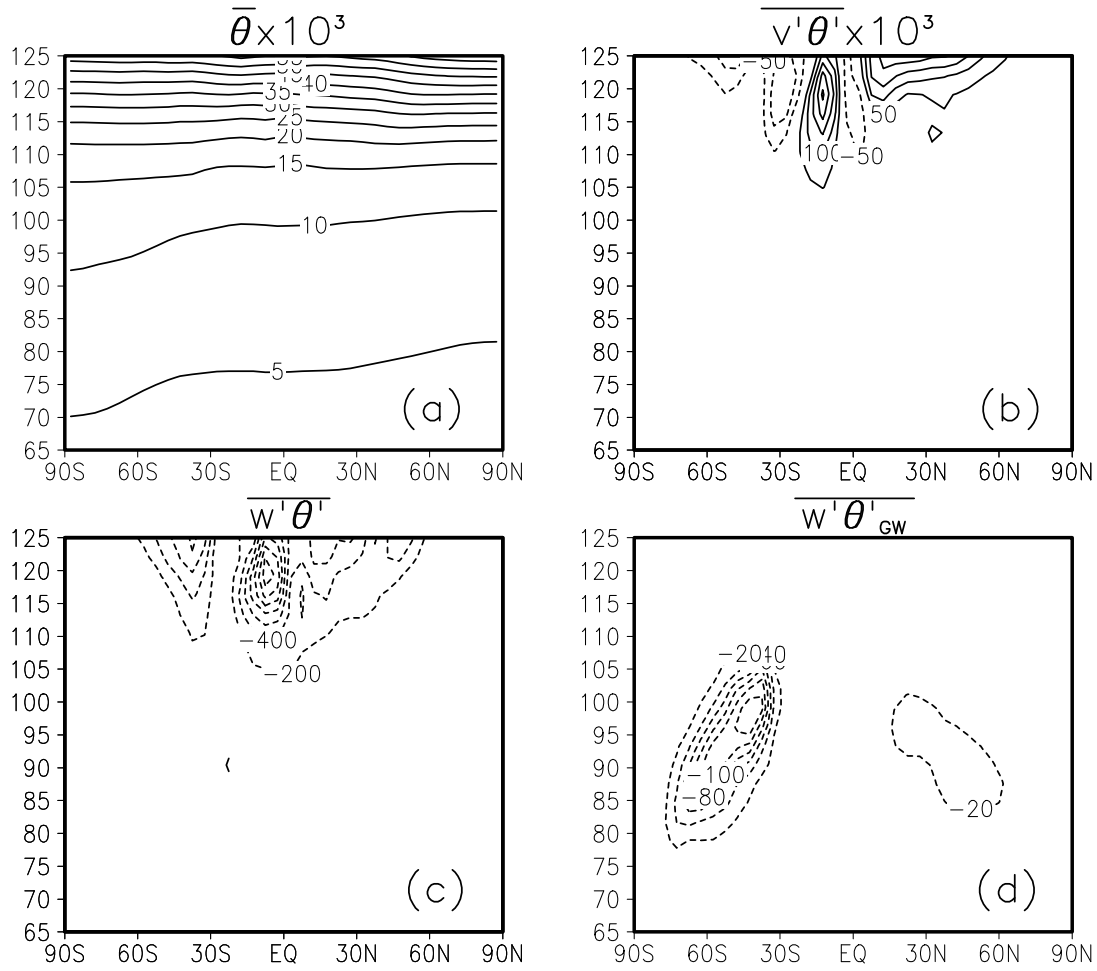


Figure 2. a) Zonal mean potential temperature in thousands of K. b) Meridional flux $\overline{v'\theta'}$ due to resolved eddies in thousands of $\text{m s}^{-1}\text{K}$. Contour interval is $50 \cdot 10^3 \text{ m s}^{-1}\text{K}$. c) Vertical flux $\overline{w'\theta'}$ due to resolved eddies. Contour interval is $200 \text{ m s}^{-1}\text{K}$. d) Vertical flux $\overline{w'\theta'}_{GW}$ due to parameterized subgrid-scale gravity waves. Contour interval is $20 \text{ m s}^{-1}\text{K}$.

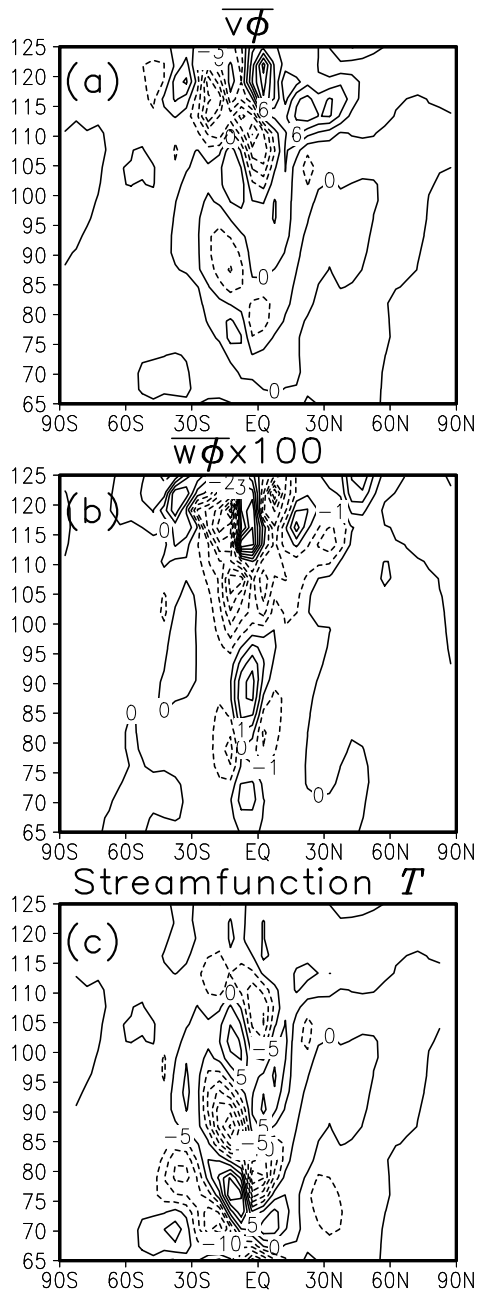


Figure 3. Meridional (a) and vertical (b) fluxes of eddy variance, $\overline{v\phi}$ and $\overline{w\phi}$, correspondingly. Contour intervals are $3 \text{ m s}^{-1}\text{K}^2$ for (a) and $0.01 \text{ m s}^{-1}\text{K}^2$ for (b). c) “Rotational” streamfunction T .

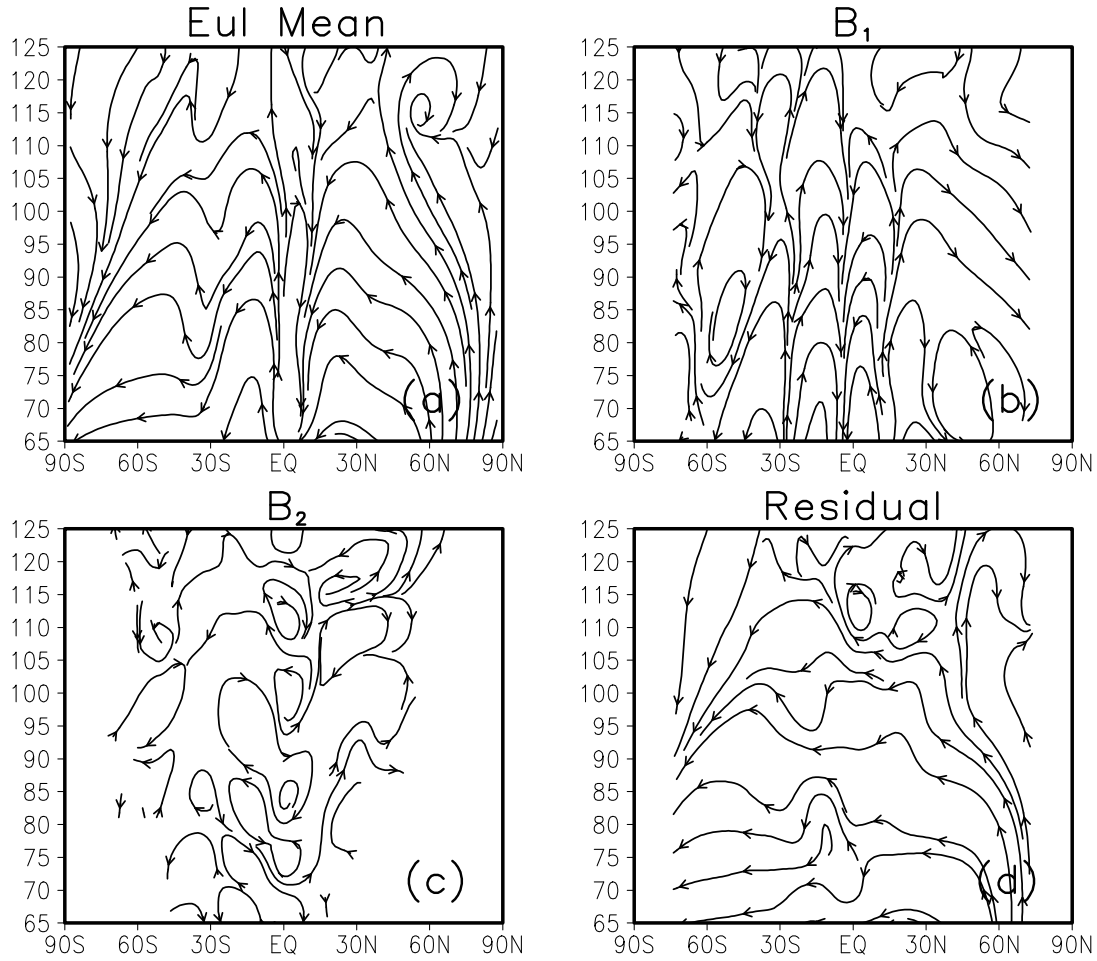


Figure 4. Height-latitude cross-sections of the advective streamfunctions: (a) due to the Eulerian-mean advection (B_{Eul}); (b) due to the eddy fluxes $\rho_0 \overline{\mathbf{v}'\theta'}$, B_1 ; (c) due to the rotational fluxes associated with $\rho_0 \overline{\mathbf{v}\phi}$, B_2 ; (d) the total residual transport streamfunction, $\bar{B} + B_1 + B_2$.

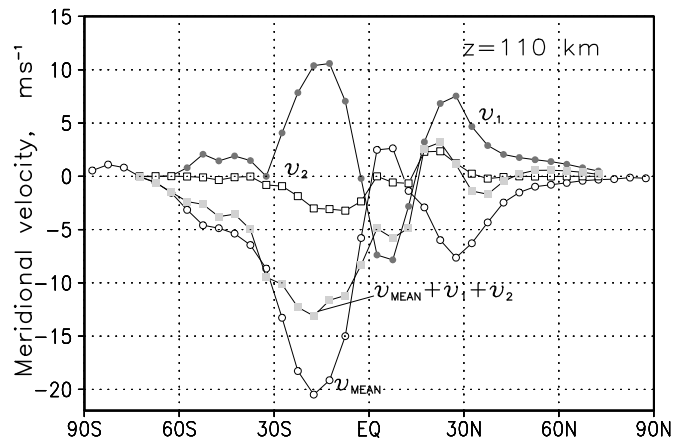


Figure 5. Components of the meridional velocity calculated from (24) and (25) at $z = 110$ km.

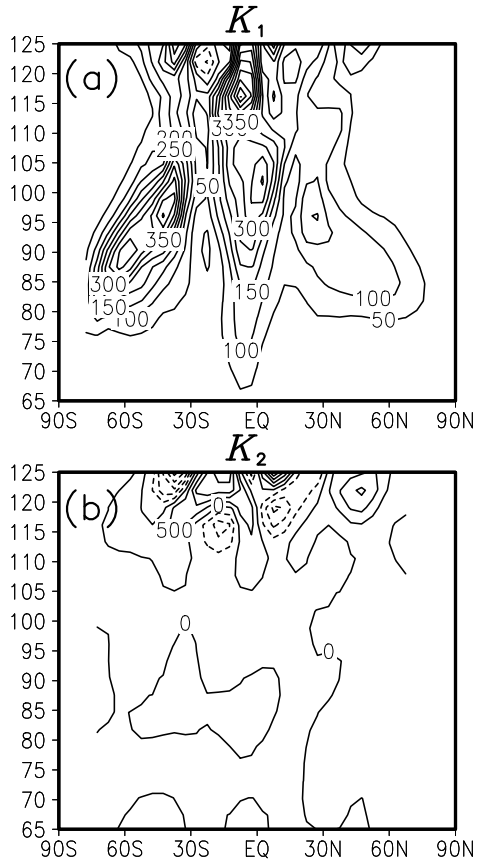


Figure 6. Components a) K_1 and b) K_2 of the diffusion coefficient calculated using (26). Contour intervals are $100 \text{ m}^2\text{s}^{-1}$ for (a) and $500 \text{ m}^2\text{s}^{-1}$ for (b).

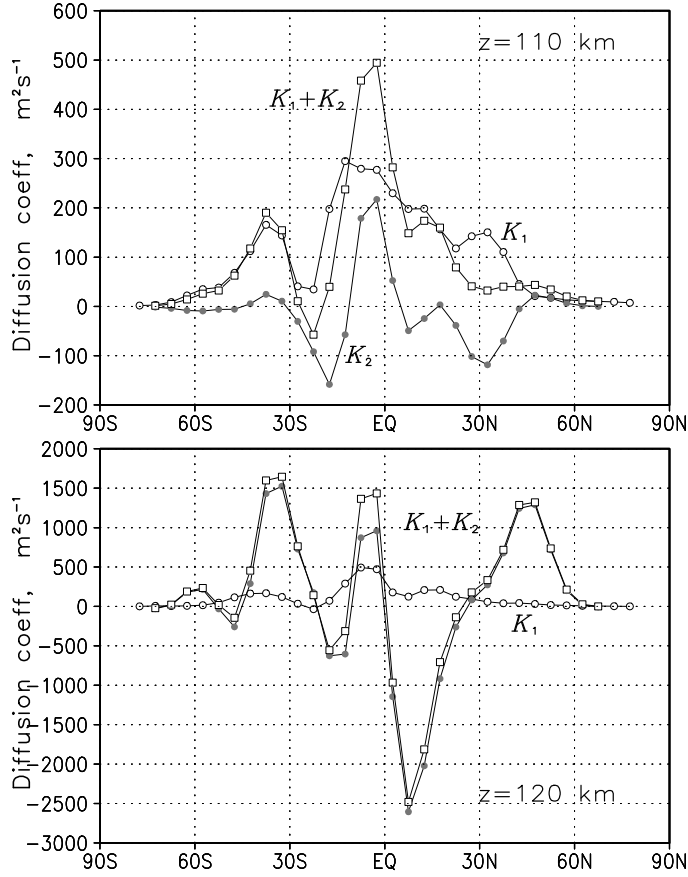


Figure 7. Latitudinal cross-sections of the diffusion coefficient K and its components, K_1 and K_2 , at a) $z=110$ km and b) $z=120$ km.

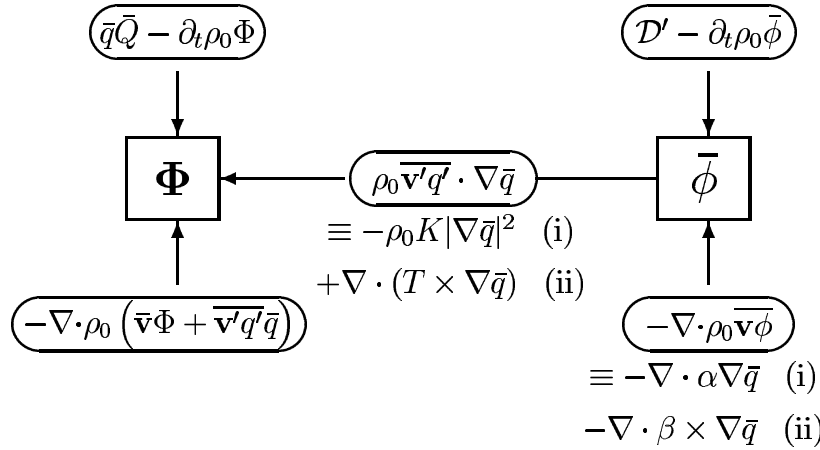


Figure 8. A schematic representation of the tracer variance cycle (6) and (7). The reservoirs Φ and $\bar{\phi}$ respectively represent mean and eddy variances of a tracer in an infinitesimal volume dV . The direction of the arrows correspond to positive values of the terms they denote.